Propagation of Ion Waves in Weakly Ionized Gases

G. M. SESSLER AND GARY A. PEARSON†
Bell Telephone Laboratories, Murray Hill, New Jersey
(Received 22 May 1967)

Theoretical and experimental results are presented on the propagation of longitudinal ion waves in weakly ionized gases in a frequency range extending from considerably below to well above the ion plasma frequency. The theory describes propagation in a uniform plasma on the basis of kinetic equations. First, a dispersion relation is derived and solved for the complex propagation constant; this is appropriate if the damping is weak. Second, the spatial dependence of the phase and amplitude of the disturbance excited by a pair of grids is calculated; when the damping is not weak, the amplitude does not decay exponentially with distance. The measurements are performed with grid-excited ion waves at frequencies between 0.1 and 10 MHz in hydrogen, nitrogen, argon, and krypton rf discharges with charged-particle densities of about 10^9 cm^{-3} and electron temperatures of the order of 50 000°K. At frequencies well below the ion plasma frequency ω_i, the phase velocity is found to be frequency-independent and is given by the Tonks-Langmuir speed. At these frequencies, the attentuation is proportional to the neutral gas pressure and is therefore primarily caused by ion-neutral collisions. At frequencies approaching ω_i, the attentuation is higher than expected from collisions, and the excess is attributed to ion Landau damping. Theory and experiment agree well at ω smaller than ω_i. For frequencies greater than ω_i, the phase velocity increases with frequency, but not as much as expected on the basis of a Maxwellian velocity distribution of the ion gas. Moreover, the ratio of imaginary to real part of the propagation constant, which is found to decrease slightly with frequency, is much smaller than expected from the theory. Better agreement between experiment and theory in this frequency range can be obtained by assuming the ionic velocity distribution to decrease more rapidly at high velocities than a Maxwellian distribution. Non-Maxwellian velocity distributions of this kind are actually expected under the conditions of the experiment. The data reported in this paper furnish the first experimental evidence of ion-wave propagation at frequencies greater than ω_i.

I. INTRODUCTION

LONGITUDINAL ion waves at frequencies above the ion plasma frequency ω_i differ considerably from low-frequency ion waves. The low-frequency waves are collective vibrations of the ions and electrons, and the velocity of these waves is determined by the properties of both particle species. If the temperature of the electron gas is much higher than the temperature of the ion gas, the waves are well described by the fluid theory which predicts a phase velocity

$$v_p=\left[\frac{KT_e}{m_i}\left(1-\frac{\omega^2}{\omega_i^2}\right)\right]^{1/2}. \quad (1)$$

This yields, for $\omega\ll\omega_i$, the Tonks-Langmuir velocity $(KT_e/m_i)^{1/2}$. If the ion and electron gases have comparable temperatures, the waves are, even in the absence of collisions, highly attenuated by Landau damping, and the theory has to be based on kinetic equations, such as the collisionless Boltzmann equation.

Ion waves at frequencies higher than the ion plasma frequency are oscillations of primarily the ion gas. The propagation is expected to be subject to strong Landau damping, regardless of the ratio of ion-to-electron temperature, if the ions have a Maxwellian velocity distribution. The fluid equations are inadequate to describe these waves, and one *has to* use the kinetic equations.

Numerous experimental studies on the propagation of low-frequency ion waves have been performed.[1–10] In many of these experiments, however, the cross-dimensions of the plasma were not large as compared to the wavelength, and guided rather than free waves were measured. The propagation of such waves depends critically on the boundary conditions and radial drifts imposed by the walls. While such experiments allow a study of boundary effects, they give little information about the influence of volume phenomena, such as collisions, on the propagation. In other experiments, the influence of wall effects was diminished by the application of a strong axial magnetic field. Contrary to the activity in the field of low-frequency ion waves, no measurements at frequencies higher than ω_i have been reported in the literature by other authors.[11]

In Sec. II of the present paper, we study the propagation of ion waves theoretically (1) by solving the dispersion equation for complex propagation constant

† Deceased.

[1] Y. Hatta and N. Sato, in *Proceedings of the Fifth International Conference on Ionization Phenomena in Gases, Munich, 1961* (North-Holland Publishing Company, Amsterdam, 1962), p. 478.
[2] A. Y. Wong, R. W. Motley, and N. D'Angelo, Phys. Rev. **133**, A436 (1964).
[3] G. M. Sessler, Phys. Letters **16**, 277 (1965).
[4] I. Alexeff and W. D. Jones, Phys. Rev. Letters **15**, 286 (1965).
[5] P. F. Little and H. G. Jones, Proc. Phys. Soc. (London) **85**, 979 (1965).
[6] P. J. Barrett and P. F. Little, Phys. Rev. Letters **14**, 356 (1965).
[7] F. W. Crawford and R. J. Kuhler, in *Proceedings of the Seventh International Conference on Ionization Phenomena in Gases, Belgrade, 1965* (Beograd, 1966), Vol. II, p. 326.
[8] G. M. Sessler, in *Proceedings of the Seventh International Conference on Ionization Phenomena in Gases, Belgrade, 1965* (Beograd, 1966), Vol. II, p. 322.
[9] A. Y. Wong, Phys. Rev. Letters **14**, 252 (1965).
[10] W. D. Jones and I. Alexeff, in *Proceedings of the Seventh International Conference on Ionization Phenomena in Gases, Belgrade, 1965* (Beograd, 1966), Vol. II, p. 330.
[11] G. M. Sessler, Phys. Rev. Letters **17**, 243 (1966).

and (2) by calculating the spatial dependence of the disturbance generated by a pair of grids; we will also compare the results obtained by the two methods. The second treatment is necessary when all modes are highly damped.[12] In Sec. III, measurements of the phase velocity and attenuation of ion waves are reported both for ω smaller and larger than ω_i. The waves are studied in the absence of a confining magnetic field under conditions where wall effects have no influence upon the propagation. This makes possible the study of collision and dissipation processes which are typical for the volume of the plasma rather than for its boundaries. The experimental results are discussed in Secs. III and IV.

II. THEORY

The theory discussed here is similar to previous work but is evaluated for parameters appropriate to the present experiment. We will assume that the plasma is in steady state, spatially uniform, and unaffected by the positions of the grids. The plasma is also assumed to be weakly ionized so only collisions with neutral particles are important.

1. Dielectric Function

The longitudinal dielectric function follows from the Fourier transformed Poisson equation as[13]

$$\epsilon(k,\omega)=1-\sum_\alpha \frac{4\pi\rho_\alpha(k,\omega)}{ikE(k,\omega)}, \tag{2}$$

where ρ_α is the charge density of particle species α, E is the longitudinal electric field, and k and ω correspond to a dependence $\exp(ikx-i\omega t)$. The contribution of species α to Eq. (2) may be obtained from the linearized Vlasov equation if all collisions can be ignored and amounts to

$$\frac{4\pi\rho_\alpha(k,\omega)}{ikE(k,\omega)}=\frac{\omega_\alpha^2}{k^2}\int d^3v\frac{\partial f_{0\alpha}/\partial v_x}{v_x-\omega/k}, \tag{3}$$

where $\omega_\alpha^2=4\pi n_\alpha q_\alpha^2/m_\alpha$ is the plasma frequency and $f_{0\alpha}$ the normalized (isotropic) velocity distribution function for species α. Use of Eq. (3) in Eq. (2) yields the familiar "Vlasov" dielectric function.

Equation (3) may be applied to the electrons by assuming that the electron mean free path is long compared with the wavelength. We obtain for positive k[14]

$$\frac{4\pi\rho_e(k,\omega)}{ikE(k,\omega)}\approx-\frac{\omega_e^2}{k^2}\left[\left\langle\frac{1}{v^2}\right\rangle_e+2\pi^2\frac{i\omega}{k}f_{0e}(0)\right] \tag{4}$$

if ω/k is small compared with the speeds of most electrons. The second term on the right gives Landau damping by the electrons.

To apply Eq. (3) to the ions we assume that the ion-neutral collision frequency ν_{in} is small compared with ω. Ordinarily Eq. (3) cannot be simplified by further approximations. However, if the phase velocity ω/k is large compared with the speeds of most ions, one can generate an asymptotic expansion valid for real ω and k by expanding the denominator $(v_x-\omega/k)$. We find, for positive k,[14]

$$\frac{4\pi\rho_i(k,\omega)}{ikE(k,\omega)}\cong\frac{\omega_i^2}{\omega^2}\left[1+\frac{3k^2}{\omega^2}\langle v_x^2\rangle_i+\cdots\right]+\frac{\omega_i^2}{k^2}i\pi\left[\int dv_y dv_z\frac{\partial f_{0i}}{\partial v_x}\right]_{v_x=\omega/k}. \tag{5}$$

The last term gives Landau damping by the ions which is, however, very small for $\omega/k\gg\langle v_x\rangle_i$. Thus collisional damping by the ions may be important. By using fluid equations, for example, one finds

$$\frac{4\pi\rho_i(k,\omega)}{ikE(k,\omega)}\cong\frac{\omega_i^2}{\omega(\omega+i\nu_{in})} \tag{6}$$

as the lowest approximation in this case.

By assuming a Maxwellian velocity distribution we obtain as a special case of Eq. (3)

$$\frac{4\pi\rho_\alpha(k,\omega)}{ikE(k,\omega)}=\frac{\omega_\alpha^2}{k^2a_\alpha^2}Z'\left(\frac{\omega}{ka_\alpha}\right), \tag{7}$$

where $a_\alpha=(2\theta_\alpha/m_\alpha)^{1/2}$ is the thermal speed, θ_α is the temperature (in energy units), and $Z'(\zeta)$ is the derivative of the plasma dispersion function.[15]

2. Dispersion Relations

Here we regard $\epsilon(k,\omega)=0$ as a dispersion equation relating complex $k=k_r+ik_i$ and real ω. This approach is incomplete when only highly damped modes ($k_i\approx k_r$) are found[12] but otherwise it does yield useful information.

When Landau damping is weak ($k_i\ll k_r$), we can obtain approximate formulas as follows. If we substitute the real terms on the right-hand sides of Eqs. (4) and (5) into Eq. (2), we obtain by writing θ_e' for $m_e/\langle v^{-2}\rangle_e$

$$v_p^2\approx\frac{\theta_e'}{2m_i}\left\{1-\frac{\omega^2}{\omega_i^2}+\left[\left(1-\frac{\omega^2}{\omega_i^2}\right)^2+12\frac{m_e\langle v_x^2\rangle_i}{\theta_e'}\right]^{1/2}\right\} \tag{8}$$

[12] R. W. Gould, Phys. Rev. **136**, A991 (1964).

[13] B. D. Fried, A. N. Kaufman, and D. L. Sachs, Phys. Fluids **9**, 292 (1966).

[14] One must use the causal dielectric function; in practice this means that in any integral of the form $\int dv\, a(v)/(v-\omega/k)$ the contour of integration is chosen such that the pole need not cross the contour as $\omega\to\omega+i\infty$. [We assume $a(v)$ is analytic.] This corresponds to turning on the perturbations adiabatically or to using Laplace transforms in time. Notice in particular that different analytic expressions apply for positive and negative k; $\epsilon(k,\omega)$ is not an analytic function of k.

[15] B. D. Fried and S. D. Conte, *The Plasma Dispersion Function* (Academic Press Inc., New York, 1961).

if $\langle v_x^2\rangle_i \ll v_p^2$; this requires $\omega \lesssim \omega_i$ and $m_e\langle v_x^2\rangle_i \ll \theta_e'$. For $\langle v_x^2\rangle_i = 0$, we recover Eq. (1) if we replace θ_e' by kT_e. Electron and ion Landau damping may be found, for Maxwellian velocity distributions, from Eqs. (2) and (7) by using the series and asymptotic expansions of Z', respectively. We obtain

$$\frac{k_i}{k_r} \approx \frac{\sqrt{\pi}}{D}\left[\frac{\theta_i}{\theta_e}\frac{v_p}{a_e}v + \exp(-v^{-2})\right], \tag{9}$$

where $v = a_i/v_p$ and $D = v^3(1+3v^2+\cdots-\omega^2/\omega_i^2)$. Damping by ion-neutral collisions follows by substituting Eq. (6) and the first term on the right of Eq. (4) into Eq. (2)

$$\frac{k_i}{k_r} \approx \frac{\nu_{in}}{2\omega}\frac{\theta_e'}{m_i v_p^2}. \tag{10}$$

If ω is much smaller than ω_i, $\theta_e'/m_i v_p^2$ is approximately equal to unity and thus $k_i/k_r \approx \nu_{in}/2\omega$. For small k_i/k_r, collisional and Landau damping are probably additive; we have verified this for one particular collision model.

To obtain an expression which is also valid for large ion Landau damping ($k_i \lesssim k_r$), we will assume the ionic velocity distribution to be Maxwellian and use Eq. (7) for the ions. By ignoring the second term on the right of Eq. (4) we obtain from Eq. (2)

$$\epsilon(k,\omega) = 1 - \frac{\omega_i^2}{k^2 a_i^2}Z'\left(\frac{\omega}{ka_i}\right) + \frac{\omega_e^2}{k^2}\left\langle\frac{1}{v^2}\right\rangle_e. \tag{11}$$

The dispersion relation $\epsilon(k,\omega) = 0$ can now be written as

$$Z'(\zeta) = \frac{2\theta_i}{\theta_e'} + \frac{\omega^2}{\omega_i^2}\zeta^{-2}, \quad \zeta = \frac{\omega}{ka_i}. \tag{12}$$

Notice that for ω sufficiently smaller than ω_i, the solutions ζ are constants independent of ω. For ω sufficiently larger than ω_i, the solutions ζ are independent of θ_i/θ_e' and the electrons play no role. Phase velocity $v_p = \omega/k_r$ and damping k_i/k_r, obtained from Eq. (12) for various temperature ratios, are plotted in Fig. 1 as function of frequency. The results show clearly that the damping is weak only if $\theta_i \ll \theta_e'$ and $\omega < \omega_i$. Equation (12) is most useful in the range $0.05 < k_i/k_r < 0.5$ where Eqs. (8) and (9) break down. Actually Eq. (12) has many additional solutions corresponding to highly damped modes which interfere with the least-damped mode if $k_i \approx k_r$; rather than considering all modes in detail, we will now proceed differently.

3. Inversion of Fourier Transform

To give a more complete discussion which includes a treatment of transmitting and receiving grids we follow Gould[12] and Fried, Kaufman, and Sachs.[13] We assume that the separation Δx of the two transmitting grids is small compared with the wavelength and that the same

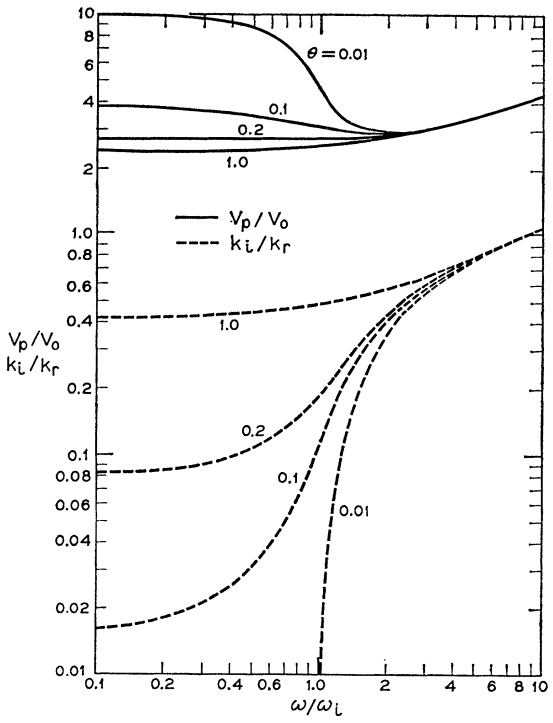

FIG. 1. Phase velocity and damping of ion waves for different temperature ratios $\theta = \theta_i/\theta_e'$. Reference quantity $v_0 = (\theta_i/m_i)^{1/2}$.

is true for the two receiving grids. We assume further that the grids intercept no particles so their effect is purely electrical.

The voltage $V_R(x,\omega)$ generated between the two receiving grids located at a distance x from the transmitting grids is given by

$$V_R(x,\omega) = V_T(\omega)\Delta x\frac{\partial R(x,\omega)}{\partial x}. \tag{13}$$

Here $V_T(\omega)$ is the voltage applied between the two transmitting grids and $R(x,\omega)$ is the response function which may be expressed as $R_1(x,\omega)+R_2(x,\omega)$ (see Appendix A) with

$$R_1(x,\omega) = -\frac{1}{\pi}\int_0^\infty \frac{dk}{k}\left[\sin kx\,\mathrm{Re}\left(\frac{1}{\epsilon(k,\omega)}\right) - \cos kx\,\mathrm{Im}\left(\frac{1}{\epsilon(k,\omega)}\right)\right], \tag{14}$$

$$R_2(x,\omega) = -\frac{1}{\pi}\int_0^\infty \frac{dk}{k}e^{ikx}\,\mathrm{Im}\left(\frac{1}{\epsilon(k,\omega)}\right). \tag{15}$$

Notice that R_1 is purely real and so cannot represent a propagating disturbance. Gould argues that R_1 consists only of exponential terms and, for Maxwellian distributions, has the form $\exp(-|x|/D)$, where D is approximately the Debye length.[12] Our primary interest is therefore in R_2. For Maxwellian distributions, Gould has evaluated R_2 for a number of cases, primarily for

$\theta_e=\theta_i$ and $\omega\ll\omega_i$. We have used Eq. (11) in evaluating R_2 for $\theta_e>\theta_i$ and $\omega\gtrsim\omega_i$. Typical results are shown in Figs. 2 and 3. The parameter $\omega x/a_i$ is chosen as abscissa since, for $\omega\ll\omega_i$, R_2 is proportional to ω^2 but otherwise depends on x and ω only through $\omega x/a_i$.[16,17]

For $\omega\lesssim\omega_i$, we obtain weakly damped exponential results for R_2 that agree well with the roots of the dispersion relation $\epsilon(k,\omega)=0$ as given in Fig. 1. In this range the dispersion relation is, however, much easier to evaluate. For $\omega\gg\omega_i$, R_2 decreases rapidly with x and does not appear exponential, although it may be dominated by two exponential terms corresponding to two highly damped roots of $\epsilon(k,\omega)=0$. The result for $\theta=0.5$ and $\omega=1.5\omega_i$ shows an interesting interference of two or more such modes.

For very large x, the evaluation of R_2 is impractical because the factor e^{ikx} oscillates so rapidly. An approximate evaluation by the saddle-point method is then appropriate. Such an evaluation (see Appendix B) yields for $\omega\gg\omega_i$ and for a Maxwellian velocity distribution of the ions

$$R_2(x,\omega)\underset{x\to\infty}{\longrightarrow}\frac{2}{\sqrt{3}}\frac{1}{|\epsilon|^2}\left(\frac{\omega_i}{\omega}\right)^2\left(\frac{\omega x}{2a_i}\right)^{2/3}e^{2\pi i/3}\times\exp\left[\frac{3}{2}\left(\frac{\omega x}{2a_i}\right)^{2/3}(\sqrt{3}i-1)\right]. \quad (16)$$

For large x the spatial dependence of R_2 is dominated by the exponential factor. This yields a "phase velocity"

$$v_p\approx\left(\frac{\omega x}{2a_i}\right)^{1/3}\frac{4}{9}\sqrt{3}a_i, \quad (17)$$

which increases slowly as x and ω increase. The "attenuation" is given by

$$k_i/k_r\approx 1/\sqrt{3}. \quad (18)$$

A numerical evaluation shows that Eq. (16) agrees reasonably well with Eq. (15) (or Figs. 2 and 3) for $\omega=3\omega_i$ and $\omega=5\omega_i$ if $\omega x/a_i>20$. The results for $\omega\gg\omega_i$, as expressed in Eqs. (16) to (18), are determined by the velocity distribution of the ions, while the distribution of the electrons does not enter.

Since non-Maxwellian velocity distributions are frequently encountered in experiments it is of interest to examine how deviations from a Maxwellian will influence the results. As an example, suppose that for v_x near the phase velocity v_p, the ion velocity distribution is such that

$$\int dv_y dv_z\, f_{0i}\propto e^{-(v_x/u)^n},\quad n\geq 2. \quad (19)$$

Then one finds from the saddle-point method

$$v_p\approx\left(\frac{\omega x}{nu}\right)^{1/(n+1)}\left[\left(1+\frac{1}{n}\right)\cos\frac{\pi}{2(n+1)}\right]^{-1}u\approx\left(\frac{\omega x}{nu}\right)^{1/(n+1)}u \quad (20)$$

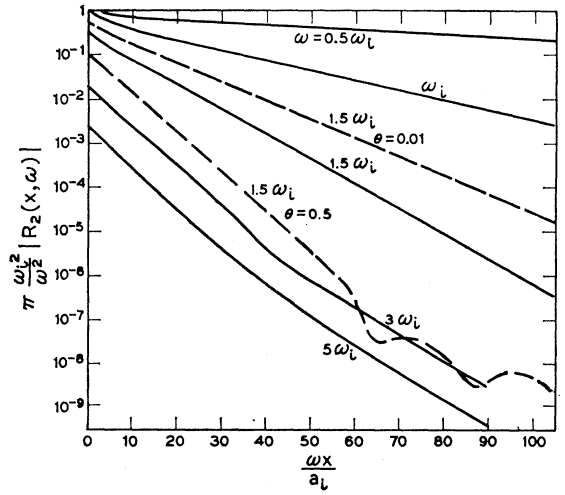

FIG. 2. Amplitude of $(\omega_i/\omega)^2\pi R_2(x,\omega)$ as a function of the distance x from the transmitting grids. The solid curves are for $\theta\equiv\theta_i/\theta_e'=0.1$ and various values of ω/ω_i. The dashed curves are for $\omega=1.5\,\omega_i$ and various values of θ. For $\omega>3\omega_i$, the results depend very weakly on θ, particularly for $\theta<0.2$.

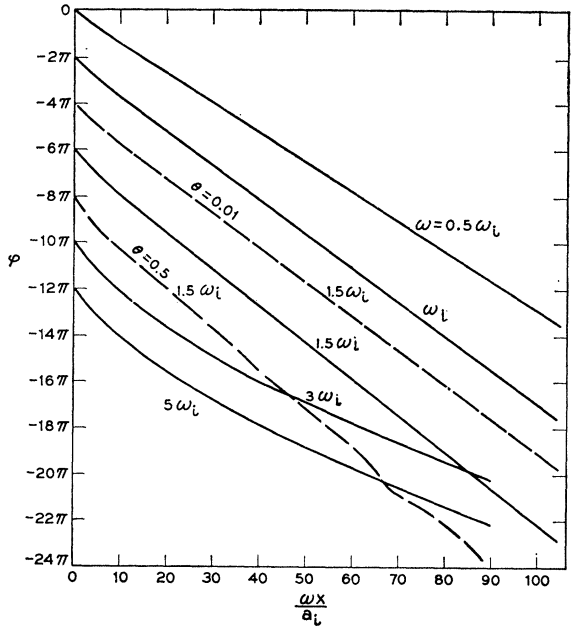

FIG. 3. Phase φ of $-R_2(x,\omega)\equiv|R_2(x,\omega)|e^{-i\varphi}$. The caption for Fig. 2 applies. For clarity, the curves have been displaced vertically.

[16] This may be seen from Eqs. (11) and (15) after changing variables to $\eta=ka_i/\omega$.

[17] Thus, Eq. (13) shows that at low frequencies $V_R(x,\omega)/V_T(\omega)$ is proportional to ω^3 and otherwise depends only on $\omega x/a_i$.

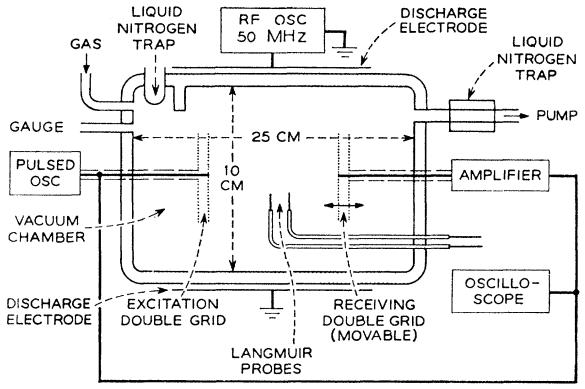

FIG. 4. Apparatus for excitation and measurement of ion waves.

and

$$\frac{k_i}{k_r} \approx \tan\frac{\pi}{2(n+1)} \approx \frac{\pi}{2(n+1)}. \tag{21}$$

This shows that for increasing n the dependence of phase velocity upon frequency and distance becomes weaker while the damping decreases.

III. EXPERIMENTAL RESULTS AND DISCUSSION

1. Experimental Method

The method for the generation and measurement of ion waves is discussed in detail elsewhere.[18] Therefore, only a brief description is given in the following.

Figure 4 shows the setup for the experiment. The plasma is generated in a glass tube by a continuous rf-discharge at a frequency of 50 MHz. Langmuir probes are used to measure the electron and ion densities and the temperature of the electron gas.

The ion waves are excited by applying pulsed wave trains with carrier frequencies between 0.1 and 10 MHz

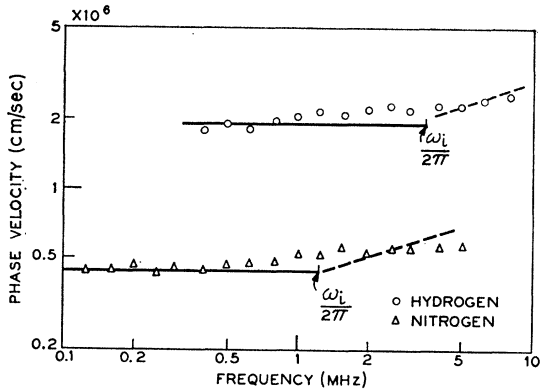

FIG. 5. Phase velocity of ion waves in hydrogen and nitrogen discharges. Plasma parameters are in Table I. Plasma frequencies ω_i are indicated. Solid and dashed lines: best fit at low and high frequencies, respectively, with the required frequency dependence.

[18] G. M. Sessler, J. Acoust. Soc. Am. 42, 360 (1967).

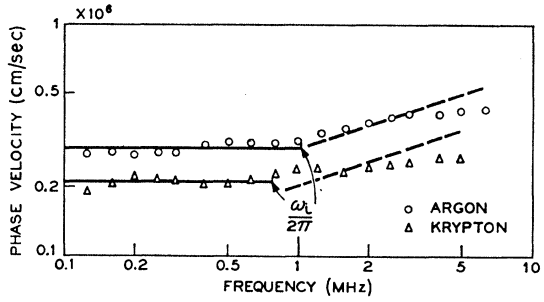

FIG. 6. Phase velocity of ion waves in argon and krypton discharges, otherwise like Fig. 5.

to a pair of parallel grids. The spacing between the two grids is 0.07 cm and the grid diameter is 5 cm.[19] Another pair of grids is employed to detect the almost cylindrical beam of waves (beam diameter equal to grid diameter). The distance between the two pairs of grids is variable, thus making the measurement of phase velocity and damping of the waves possible.

The plasma density in the cylindrical space in which the waves propagate is homogeneous to within ±10%. The inhomogeneities are, however, greater within the sheaths of the grids.[18]

2. Phase Velocity as Function of Frequency

The measured phase velocities of ion waves are plotted in Fig. 5 for the hydrogen and nitrogen discharges and in Fig. 6 for the argon and krypton discharges as a function of frequency. The plasma parameters for the four discharges are given in Table I. In all but the hydrogen plasma, about the same neutral gas pressure, charged particle density, and electron temperature are used. The temperature of the ion gas, which cannot be measured with probes, is estimated to be above room temperature by a factor of order 10. This is due to ambipolar dc fields which are, for locations not too close to the walls, about 200 to 300 V/(cm Torr).[18]

The velocity results in Figs. 5 and 6 indicate an absence of dispersion at frequencies well below $\omega_i/2\pi$, as expected from Fig. 1 or Eq. (1). A comparison between the measured phase velocities v_m at low frequencies (solid lines in Figs. 5 and 6) and those predicted by Eq. (1) is given in Table II. The ion temperature is not considered in Eq. (1). By using Eq. (8) and substituting an ion temperature of, say, 3000°K, the $(v_m/v_p)^2$ values in Table II would all be lowered by 15 to 20%. Results by Alexeff and Jones,[4] who have interpreted $(v_m/v_p)^2$ as the specific heat ratio of the electron gas, are also given in Table II. The particle densities in the experiments by Alexeff and Jones were about equal to those used in the present study.

The slight deviations of $(v_m/v_p)^2$ from unity could be

[19] Other pairs of grids with spacings between 0.05 and 2 cm and diameters between 2.5 and 6 cm yield about the same results for phase velocity and attenuation [see Ref. 18].

TABLE I. Plasma parameters.

	Hydrogen	Nitrogen	Argon	Krypton
Neutral gas pressure p_n (microns)	10	2.5	2.5	2.5
Electron and ion densities N_e and N_i (cm^{-3})	0.58×10^9	1.0×10^9	1.0×10^9	1.1×10^9
Ion plasma frequency $\omega_i/2\pi$ (MHz)	3.6	1.2	1.0	0.77
Electron gas temperature T_e (°K)	69 000	45 000	48 000	48 000

due to the fact that the electron velocity distribution is non-Maxwellian; thus the quantity θ_e' in Eq. (8), which determines the phase velocity, may not equal the "temperature" measured by a probe and used to calculate v_p.

The deviations of $(v_m/v_p)^2$ from unity may also in part be attributed[8] to a change in the effective ion mass due to the presence of more than one ion species in each plasma. The phase velocity in a plasma with several ion species having masses equal to $M_1, M_2, \cdots$ and relative densities $x_1, x_2, \cdots$ is

$$v_p' = (\theta_e')^{1/2}[(x_1/M_1)+(x_2/M_2)+\cdots]^{1/2}. \quad (22)$$

The values of $(v_m/v_p)^2$ in Table II were obtained by assuming the presence of only H_2^+, N_2^+, Ar^+, and Kr^+, respectively. If we assume that H^+, N^+, Ar_2^+, and Kr_2^+ are also present in the respective cases, $(v_m/v_p)^2$ is decreased for hydrogen and nitrogen but is increased for argon and krypton.

In the presence of a second considerably heavier ion species, another ion wave with a lower speed may exist under certain conditions. Experiments in nitrogen-mercury mixtures actually show the propagation of two ion waves having a phase velocity ratio of about 1:4. The phase velocity of the faster wave is equal to that

TABLE II. Experimental results.

	Hydrogen	Nitrogen	Argon	Krypton
$(v_m/v_p)^2$ at $\omega\ll\omega_i$	1.20	1.45	0.85	0.90
γ_e from Alexeff and Jones[a]	···	···	1.00	0.81
T_i (°K) from phase velocity at $\omega>\omega_i$	8500	3300	2000	1400
T_i (°K) from attenuation at $\omega<\omega_i$	10 500	4500	4000	4800
$\nu_{in}(sec^{-1})$ at 1 Torr from attenuation data	···	···	5×10^7	···

[a] See Ref. 4.

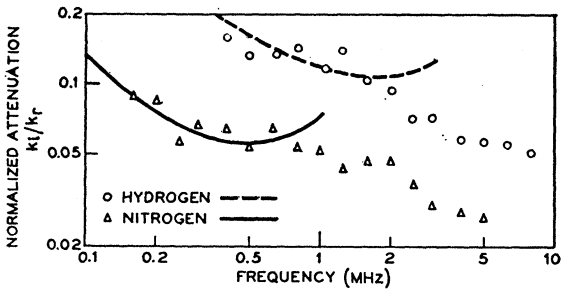

FIG. 7. Normalized attenuation k_i/k_r of ion waves in hydrogen and nitrogen discharges. Plasma parameters are in Table I. Theoretical curves: sum of expected collisional and ion Landau damping.

expected for a nitrogen plasma. Ion waves behave in this respect differently than ordinary sound waves where the particle species are strongly coupled by collisions, thus permitting only one wave to propagate.

At frequencies higher than ω_i, Figs. 5 and 6 indicate a slight increase of the phase velocities. As shown in Sec. II 3, the kinetic theory predicts the phase velocity and damping to depend in this case on the separation x between the two pairs of grids. Since the measurements at $\omega>\omega_i$ were taken at values of $\omega x/a_i$ between 60 and 800, it is appropriate to compare the experimental results with the asymptotic solutions given in Eqs. (17) and (20). The dashed lines in Figs. 5 and 6 have the dependence on $\omega^{1/3}$ predicted by Eq. (17) but are otherwise best fits to the data. The observed dependence on ω is apparently somewhat more gradual than predicted by the theory based on a Maxwellian velocity distribution of the ions. This indicates that the velocity distribution in the experiment corresponds to $n>2$ in Eqs. (19) and (20). The fact that the phase velocity measurements yield[18] values independent of x also seems to suggest a relatively large exponent in Eq. (20). We will deal with these questions in more detail when we discuss the damping measurements in Sec. III 3.

The ion temperatures derived from the dashed lines in Figs. 5 and 6 are given in Table II. A separation $x=2.5$ cm, corresponding to the center of the measuring interval (2 to 3 cm at high frequencies), has been used for the evaluation.

3. Attenuation as Function of Frequency

The normalized attenuation constant is shown in Fig. 7 for the hydrogen and nitrogen discharges and in Fig. 8 for the argon and krypton discharges. The plasma parameters are the same as for the velocity measurements (see Table I).

The expected attenuation consists of damping due to ion-neutral collisions and of ion Landau damping. Electron Landau damping is, for the temperature ratios T_i/T_e under consideration, much smaller than ion Landau damping. The lines in Figs. 7 and 8 represent the expected total damping, calculated with Eqs.

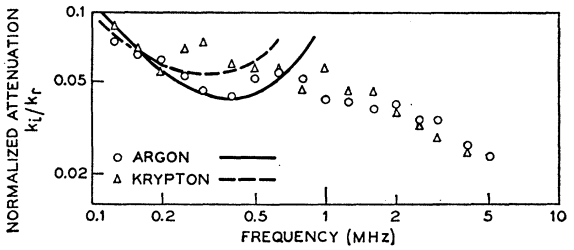

FIG. 8. Normalized attenuation k_i/k_r of ion waves in argon and krypton discharges, otherwise like Fig. 7.

(10) and (12) under the assumption that collisional and Landau damping are additive (see Sec. II). For the calculations, known collision cross sections for dc fields of 300 V/(cm Torr) (see above) are used, while the ratio T_i/T_e is adjusted to yield best fit with the data. The resulting T_i values are shown in Table II and may be compared with the ion temperatures derived from the velocity measurements at $\omega > \omega_i$. These determinations of T_i rely, of course, on the assumption of a Maxwellian velocity distribution of the ion gas and are thus not expected to be very accurate.

If ω is raised above ω_i, the attenuation is primarily caused by ion Landau damping. For well above ω_i and for large transmitter-receiver separations the damping is expressed by Eq. (18) if a Maxwellian velocity distribution of the ion gas is assumed. The observed attenuation is by about an order of magnitude smaller. This suggests again that the experimental velocity distribution of the ions corresponds to $n > 2$ in Eqs. (19) and (21), thus yielding lower damping. For k_i/k_r to be as small as the experimental value, one would have to choose $n \gtrsim 20$. This suggests that an ion velocity distribution with a sharp cutoff is needed to explain the experimental results. This distribution, however, need not have the form given by Eq. (19). The reason for using this particular distribution is that it permits an easy evaluation. Because the ions gain their energy from the ambipolar field, a distribution with a sharp cutoff is actually expected in this experiment.

It is of interest in this context that experiments by Wong[9] yielded also much smaller ion Landau damping than predicted on the basis of a Maxwellian velocity distribution of the ions. Wong's experiments were made in a highly ionized plasma with $T_i \approx T_e$ at frequencies much smaller than the ion plasma frequency. A similar result has been obtained for Landau damping of electron waves by Van Hoven.[20]

4. Dependence on Neutral Gas Pressure

Variation of the neutral gas pressure offers a possibility to check whether the attenuation at low frequencies is due to ion-neutral collisions and, if this is the case, to determine the cross section for this collision process. The ratio of attenuation to pressure should be independent of frequency and pressure if ion-neutral collisions are the only reason for the damping, as is the case at very low frequencies.

Measurements of α/p_n are shown in Fig. 9 for some argon plasmas having different pressure but equal ion density of 1.3×10^9 cm^{-3}. Also shown are theoretical curves representing the sum of collisional and ion Landau damping. Since ω is much smaller than ω_i, the collisional part of the attenuation follows from Eq. (10) by setting $\theta_e'/(m_i v_p^2)$ equal to unity. It is therefore given by $(k_i)_{\text{coll}} = \nu_{\text{in}}/2v_p$. Ion Landau damping may be determined with Eq. (12) (or from Fig. 1) for known temperature ratio T_i/T_e. The curves shown in Fig. 9 are obtained by substituting the measured phase velocity of 3×10^5 cm/sec (which is independent of pressure and frequency in the ranges under consideration) and by treating ν_{in} and T_i/T_e as disposable parameters. This yields, for a pressure of 1 Torr, $\nu_{\text{in}} = 5\times10^7$ sec^{-1}, in agreement with the value expected[21] from drift velocity measurements assuming $E/p_n = 300$ V/(cm Torr). The corresponding collision cross section $Q_m = \nu_{\text{in}}/a_i N_n$ is, for $a_i = 1.7\times10^5$ cm/sec, equal to 0.83×10^{-14} cm^2. The fitted temperature ratio follows as $T_e/T_i = 12$, which agrees with that obtained from the data in Fig. 8. The curves shown in Fig. 9 approach the collisional damping value asymptotically with decreasing frequency.

The fact that the observed attenuation per Torr is independent of frequency and pressure at the lower frequencies indicates that damping due to ion-neutral collisions dominates in this range. This is substantiated by the result that the ion-neutral collision frequency derived from the attenuation measurements agrees with that obtained by other methods.

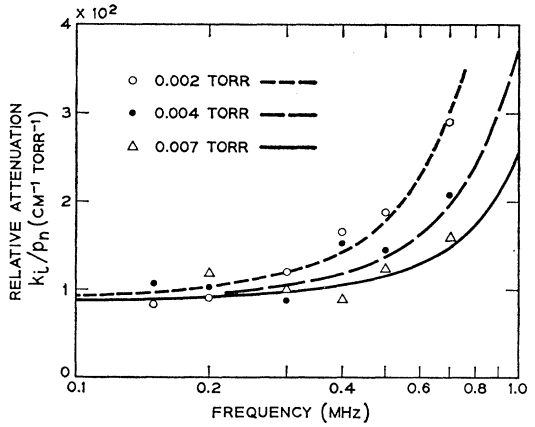

FIG. 9. Relative attenuation k_i/p_n of ion waves in argon discharges ($n_e = 1.3\times10^9$ cm^{-3}) at various neutral gas pressures. The lines represent the sum of expected collisional and ion Landau damping.

[20] G. Van Hoven, Phys. Rev. Letters **17**, 169 (1966).

[21] J. A. Hornbeck, Phys. Rev. **84**, 615 (1951).

5. Excitation Coefficient

The measured over-all frequency response of the ion wave experiment is shown in Fig. 10. The results are obtained by feeding a frequency-independent voltage into the excitation grid and measuring the voltage produced by the receiving grid as a function of frequency. Since measurements are not possible for zero separation between excitation and receiving grids, the amplitude-versus-separation dependence measured at distances from 2–6 cm is extrapolated to zero separation. The results are shown in Fig. 10.

The solid line in Fig. 10 is the predicted dependence calculated for zero separation between excitation and receiving grids. For low frequencies, the theory yields[17] a dependence proportional to ω^3. The dependence is weaker at frequencies comparable to or higher than ω_i. The agreement between the measured and the predicted dependence on frequency is good.

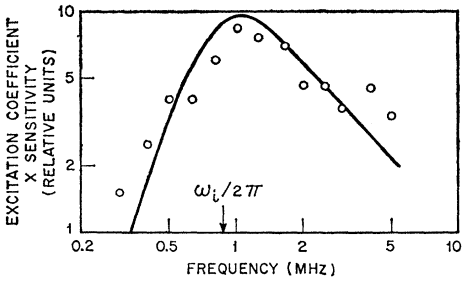

FIG. 10. Excitation coefficient times sensitivity in a nitrogen plasma. Solid line: expected dependence for $\theta_i/\theta_e'=0.1$, with $\omega_i/2\pi=0.87$ MHz. This effective plasma frequency is smaller than the value 1.1 MHz measured by probes at the plasma center, presumably because it represents a spatial average.

IV. DISCUSSION

In deriving our theoretical model, a number of assumptions about the plasma and the grids have been made. We would like to discuss now whether these assumptions are in agreement with the experimental conditions.

The plasma can certainly be assumed to be in steady state since the rf fields that maintain the discharge have little effect upon wave propagation which occurs at much lower frequencies. Similarly, the assumptions about the various collision rates are known to be valid.

The assumption concerning the grid spacing is a good approximation for most of the frequency range under consideration since separations Δx as small as 0.05 cm were used while the shortest wavelength is about 0.07 cm. With variable grid separations,[19] only an effect on the amplitude of the disturbance, but not on its phase velocity and attenuation, could be detected experimentally.[18] The assumption that the grids intercept no particles is expected to affect also primarily the amplitude of the disturbance excited and should again be of little importance to the propagation.

It is apparent from the geometry of the grid structures that one expects longitudinal waves propagating directly from the transmitting to the receiving grids. Any other path would involve higher attenuation and would not yield the observed linear dependence of phase on separation.[18] Since the wavelength is small compared with the grid diameter, one expects a well-defined beam of nearly plane waves.

By using Eq. (11) in evaluating $R_2(x,\omega)$, we have assumed effectively massless electrons. This overlooks an additional contribution to R_2 that was investigated by Gould.[12] However, this contribution represents a disturbance that propagates with a much higher speed, characteristic of electron speeds, and so appears temporally separated from the ion-wave signal in experiments with pulsed wave trains.

We expect no great effect from the plasma-density inhomogeneity,[18] which is due to wall effects. The relatively great inhomogeneity near the grids can be regarded as part of the grid structure and will affect only the efficiency of the grids, while the small inhomogeneity of the plasma density elsewhere in the region of the wave propagation has a scale length long compared with the wavelength. Furthermore, the phase velocity depends only weakly on the plasma density.

Radial drifts, which are also due to wall effects, tend to extract ions and electrons from the wave beam. Note that if one particle leaves the beam and is replaced by another, the effect is similar to that of a collision.[18] Because in the experiment the collision mean free path for ions is shorter than the beam diameter, one expects little effect from radial drifts of the ions. Since the electrons store no appreciable momentum, their drifts are of no influence on the wave motion even though their mean free path is comparable to the beam diameter.

The wall effects give rise to ambipolar electric fields that could lead to distorted velocity distributions because the apparatus dimensions are not very much greater than the particle mean free paths. Actually, the electrons are "contained" by the ambipolar field long enough to suffer many collisions, so the electron velocity distribution should not be seriously anisotropic. No similar reasoning applies for the ion velocity distribution, which may be highly distorted and certainly cannot be assumed to be Maxwellian.

V. SUMMARY AND CONCLUSIONS

The experimental results obtained at frequencies *smaller* than the ion plasma frequency agree well with theory. Of particular interest are the wave-attenuation data which yield information on dissipation phenomena due to volume effects in weakly ionized gases, a rather unexplored field from an experimental point of view. It is found that the attenuation at frequencies well below ω_i is caused by ion-neutral collisions; the corresponding collision frequency for momentum transfer agrees with that determined from mobility measure-

ments. At frequencies below but close to ω_i the attenuation is higher than expected from collisions and the excess is attributed to ion Landau damping. The phase velocity, which is frequency-independent, is determined by the Tonks-Langmuir relation as has also been found by other authors.

The data taken at frequencies *larger* than the ion plasma frequency represent the first experimental proof of ion-wave propagation in this range. The measurements, which were performed at transmitter-receiver separations much larger than the wavelength, show a small increase of the phase velocity and a slight decrease of the normalized attenuation constant with frequency. These results require the assumption of an ion velocity distribution which decreases more rapidly than a Maxwellian at high velocities. Non-Maxwellian velocity distributions of this kind are expected under the conditions of the experiment.

As has been implied in this paper, ion waves have many potential applications in plasma diagnostics. Contrary to probe measurements, experiments on such waves allow one to determine many parameters without disturbing the plasma. Phase velocity and attenuation at low frequencies, for example, yield the electron temperature and the ion-neutral collision cross section, respectively, while measurements at frequencies comparable to and above the ion plasma frequency give information about the average ion temperature and the shape of the ionic velocity distribution.

ACKNOWLEDGMENTS

The authors are grateful to Dr. P. A. Wolff for many helpful discussions. Thanks are also due to J. H. Kronmeyer for aid in mechanical design.

APPENDIX A

The electric field at a distance x from the transmitting grids is given by

$$E(x,\omega)=V_T(\omega)\int_{-\infty}^{\infty}\frac{dk}{2\pi}\frac{e^{ikx}}{\epsilon(k,\omega)}, \tag{A1}$$

where $V_T(\omega)$ is the voltage between the transmitting grids. The voltage between the receiving grids at position x is then $V_R(x,\omega)=\Delta x\, E(x,\omega)$, which we prefer to write as

$$V_R(x,\omega)=V_T(\omega)\Delta x\frac{\partial R(x,\omega)}{\partial x}, \tag{A2}$$

where

$$R(x,\omega)=\int_{-\infty}^{\infty}\frac{dk}{2\pi}\frac{e^{ikx}}{ik\epsilon(k,\omega)}. \tag{A3}$$

If this is regarded as a contour integral in the complex k plane, one may close the contour in the upper half plane for positive x. Then poles of $\epsilon(k,\omega)$ [solutions of $\epsilon(k,\omega)=0$] in the upper half of the complex k plane yield exponential contributions to $R(x,\omega)$; in addition, because $\epsilon(k,\omega)$ has a branch cut,[14] there is a nonexponential contribution to $R(x,\omega)$.

If $V_T(t)$ can be Fourier transformed, we need only to evaluate $R(x,\omega)$ for real ω. If $\epsilon(k,\omega)$ is an even function of k for real k,[13] we may write for Eq. (A3)

$$R(x,\omega)=\frac{1}{\pi}\int_0^{\infty}\frac{dk}{k}\frac{\sin kx}{\epsilon(k,\omega)}. \tag{A4}$$

$R(x,\omega)$ can be expressed as $R_1(x,\omega)+R_2(x,\omega)$, with R_1 and R_2 given by Eqs. (14) and (15).

APPENDIX B

To apply the saddle-point method to $R_2(x,\omega)$, we first rewrite Eq. (15) by using Eq. (11) and substituting the imaginary part of Z' from the power series[15] to obtain

$$R_2(x,\omega)=-\frac{2}{\sqrt{\pi}}\left(\frac{\omega_i}{\omega}\right)^2\int_0^{\infty}\frac{dk}{k}\left(\frac{\omega}{ka_i}\right)^3|\epsilon(k,\omega)|^{-2}\times\exp\left[ikx-\left(\frac{\omega}{ka_i}\right)^2\right]. \tag{B1}$$

We consider $k^4|\epsilon(k,\omega)|^2$ to vary slowly with k; this is the case for $\omega\gg\omega_i$ if we use $\epsilon(k,\omega)$ as given in Eq. (11). According to the saddle-point method, the major contribution to the integral is from

$$k\approx k_0=\left(\frac{2a_i}{\omega x}\right)^{1/3}\left(\frac{\omega}{a_i}\right)e^{i\pi/6}. \tag{B2}$$

For large x this is small compared with ω/a_i so one may use

$$\epsilon\cong 1-\frac{\omega_i^2}{\omega^2}+\frac{\omega_i^2}{\omega^2}\frac{2\theta_i}{\theta_e'}\left(\frac{\omega x}{2a_i}\right)^{2/3}e^{-i\pi/3}, \tag{B3}$$

which has various limiting forms depending upon ω_i/ω, θ_i/θ_e', and x. The saddle-point method then yields

$$R_2(x,\omega)\underset{x\to\infty}{\longrightarrow}\frac{2}{\sqrt{3}}\frac{1}{|\epsilon|^2}\left(\frac{\omega_i}{\omega}\right)^2\left(\frac{\omega x}{2a_i}\right)^{2/3}e^{2\pi i/3}\times\exp\left[\frac{3}{2}\left(\frac{\omega x}{2a_i}\right)^{2/3}(\sqrt{3}i-1)\right]. \tag{B4}$$

Similar results are known for electron waves.[12]